



Queensland University of Technology
Brisbane Australia

This is the author's version of a work that was submitted/accepted for publication in the following source:

Frost, Ray L., Williams, Peter, Martens, Wayde N., Leverett, Peter, & Klopogge, J. Theo (2004) Raman spectroscopy of basic copper(II) and some complex copper(II) sulfate minerals: Implications for hydrogen bonding. *American Mineralogist*, 89(7), pp. 1130-1137.

This file was downloaded from: <http://eprints.qut.edu.au/22094/>

© Copyright 2004 Mineralogical Society of America

Notice: *Changes introduced as a result of publishing processes such as copy-editing and formatting may not be reflected in this document. For a definitive version of this work, please refer to the published source:*

**Raman spectroscopy of basic copper (II) and some complex copper(II) sulphate
minerals implications for hydrogen bonding**

**Ray L. Frost^{*}, Peter A. Williams^{*}, Wayde Martens, Peter Leverett^{*} and J. Theo
Kloprogge**

Centre for Instrumental and Developmental Chemistry, Queensland University of
Technology, GPO Box 2434, Brisbane Queensland 4001, Australia.

^{*}School of Science, Food and Horticulture, University of Western Sydney,
Locked Bag 1797, Penrith South DC NSW 1797, Australia.

Abstract

Raman spectroscopy has been applied to the study of basic copper sulphates including antlerite, brochantite, posnjakite, langite and wroewulfeite and selected complex copper sulphate minerals. Published X-ray diffraction data were used to estimate possible hydrogen bond distances for the basic copper sulphate minerals. A Libowitzky empirical expression was used to predict hydroxyl stretching frequencies and agreement with the observed values was excellent. This type of study was then extended to complex basic copper sulphates: cyanotrichite, devilline, glaucocerinite, serpierite and ktenasite. The position of the hydroxyl stretching vibration was used to estimate the hydrogen bond distances between the OH and the SO₄ units. The variation in bandwidth of the OH stretching bands provided an estimate of the variation in these hydrogen bond distances. By plotting the hydrogen bond O...O distance as a function of the position of the SO₄ symmetric stretching vibration, the position of the SO₄ symmetric stretching band was found to be dependent upon the hydrogen bond distance for both the basic copper sulphates and the complex copper sulphates.

^{*} Author for correspondence (r.frost@qut.edu.au)

Keywords: antlerite, brochantite, posnjakite, langite, devilline, cyanotrichite, glaucocerinite, serpierite, ktenasite, hydrogen bond, Raman spectroscopy

INTRODUCTION

Studies of the basic copper sulphate minerals have been in existence for some time (Fowles, 1926; Richmond and Wolfe, 1940; Ungemach, 1924). Such minerals are formed under specific conditions of pH and sulphate ion concentration. The minerals in this group are dolerophanite Cu_2OSO_4 (Richmond and Wolfe, 1940), antlerite $\text{Cu}_3\text{SO}_4(\text{OH})_4$ (Araki, 1961; Finney and Araki, 1963), brochantite $\text{Cu}_4\text{SO}_4(\text{OH})_6$ (Helliwell and Smith, 1997), posnjakite $\text{Cu}_4\text{SO}_4(\text{OH})_6 \cdot \text{H}_2\text{O}$, langite $\text{Cu}_4\text{SO}_4(\text{OH})_6 \cdot 2\text{H}_2\text{O}$, wroewulfite $\text{Cu}_4\text{SO}_4(\text{OH})_6 \cdot 2\text{H}_2\text{O}$ (Pollard et al., 1990). Antlerite is more stable under acidic conditions compared with brochantite. The temperature of crystallisation is significant in the synthesis of these minerals with posnjakite formed at lower temperatures than brochantite.

The principal interest in these minerals is many fold:

- (a) the study of possible materials for the restoration of frescoes (Bersani et al., 2001)
- (b) the studies of the corrosion and restoration of copper and bronze objects (Kratschmer et al., 2002; Livingston, 1991; Lobnig et al., 1999; Mankowski et al., 1997; Matsuda et al., 1997; Nord et al., 1998) (Bouchard-Abouchacra, 2001)
- (c) The corrosion of copper pipes containing reticulated water
- (d) The formation of these types of minerals in volcanic sublimations (Vergasova et al., 1988; Vergasova et al., 1984)
- (e) The formation of these types of minerals as leachates from slag dumps (Ruesenberg and Paulis, 1996; Wappler and Tischendorf, 1980).

Recent work by Bouchard- Abouchacra using Raman microscopy identified the presence of brochantite and antlerite on the corroded surface of a bronze object (Bouchard-Abouchacra, 2001). Bouchard- Abouchacra showed and was able to distinguish the minerals malachite, azurite, brochantite and antlerite (Bouchard-

Abouchacra, 2001). Other minerals can be formed during copper and lead corrosion. These include nakaurite ($\text{Cu}_4(\text{SO}_4)_4(\text{CO}_3)(\text{OH})_6 \cdot 48\text{H}_2\text{O}$), and the mixed Cu-Pb species such as chenite ($\text{CuPb}_4(\text{SO}_4)_2(\text{OH})_6$), elyite ($\text{CuPb}_4(\text{SO}_4)(\text{OH})_8$), and caledonite ($\text{Cu}_2\text{Pb}_5(\text{SO}_4)_3(\text{OH})_6$) (Bouchard-Abouchacra, 2001). Other minerals such as chalcocyanite (CuSO_4) and dolerophanite (Cu_2OSO_4) will not form in any atmosphere containing moisture. These minerals may form in for example volcanic eruptions such as with Vesuvius in 79 AD.

Many complex copper(II) sulphate systems exist with quite complex stoichiometry (Effenberger, 1985; Effenberger, 1988; Effenberger and Zemann, 1984). The complexity of these minerals results from the assembly of a wide range of cations in the structure (Giuseppetti and Tadini, 1987; Hess et al., 1988; Mellini and Merlino, 1978; Mereiter, 1982). This complexity is reinforced by the many multi-anion species incorporated in the structure. These include nitrate, phosphate, arsenate, carbonate and hydroxyl (Orlandi and Perchiazzi, 1989; Pierrot and Sainfeld, 1961; Von Hodenberg et al., 1984; Zubkova et al., 2002).

Recently the authors have applied Raman spectroscopy in a study of minerals containing oxyanions, including the elucidation of the structures of some basic copper phosphate and sulphate minerals (Frost et al., 2002b). The single crystal Raman spectra of azurite have been obtained (Frost et al., 2002a). The Raman spectra of the descloizite series and mottramite were obtained at 298 and 77 K (Frost et al., 2001). Raman spectroscopy has also been used to study the mixed anionic mineral chillagite (Crane et al., 2002). Further the vibrational spectra of some naturally occurring pseudoalums has been determined (Frost et al., 2000; Kloprogge et al., 2001). Recently, the Raman spectroscopy of the vivianite phosphates and sulphates has been undertaken. It has proven extremely powerful for studying hydrated (such as the vivianite minerals), hydroxylated (basic copper sulphates and phosphates) sulphated (natural alums) minerals. It seems apparent that few if any comprehensive Raman studies have been undertaken on these basic copper sulphate and complex basic copper sulphate minerals. The objective of this research is the study of the relationship between hydrogen bond distances and the position of the SO_4 and OH stretching vibrations in the Raman spectra of the selected sulphates.

EXPERIMENTAL

Minerals:

Langite	sample D4379	from Cornwall, United Kingdom
Brochantite	sample D20320	from Chuquicamata, Chile
Brochantite	sample D28957	from Bisbee, Arizona, USA
Antlerite	sample M33489	from Antlerite, Chuquicamata, Chile
Posnjakite	sample M27302	from Drakewalls adit, near Gunnislake, Cornwall, UK
Wroewolfeite	Univ. of Cardiff,	Wales
Cyanotrichite	sample G14601	Maid of Sunshine Mine, Cochise County, Arizona, USA.
Devilline	sample G17182	Spania Dolina, Czechoslovakia
Ktenasite	sample G24983	Glomsevo Kollen, Amot Modum, Norway
Serpierite	sample G4034	Laurium, Greece
Glaucocerinite	sample G17641	Maid of Sunshine Mine, Cochise County, Arizona, USA.

The sample number is the registered museum mineral number. The samples were phase analyzed using X-ray diffraction and the compositions checked using EDX measurements. No elements heavier than oxygen other than sulphur and copper were detected (apart from calcium for devilline).

Raman microprobe spectroscopy

The crystals of the minerals were placed and orientated on a polished metal surface on the stage of an Olympus BHSM microscope, which is equipped with 10x and 50x objectives. The crystals were oriented to provide maximum intensity. All crystal orientations were used to obtain the spectra. Power at the sample was measured as 1 mW. The incident radiation was scrambled to avoid polarisation effects. The

microscope is part of a Renishaw 1000 Raman microscope system, which also includes a monochromator, a filter system and a Charge Coupled Device (CCD). Raman spectra were excited by a Spectra-Physics model 127 He-Ne laser (633 nm) at a nominal resolution of 4 cm^{-1} in the range between 100 and 4000 cm^{-1} . Repeated acquisitions using the highest magnification were accumulated to improve the signal to noise ratio in the spectra. Spectra were calibrated using the 520.5 cm^{-1} line of a silicon wafer. Spectroscopic manipulation such as baseline adjustment, smoothing and normalisation were performed using the Spectracalc software package GRAMS (Galactic Industries Corporation, NH, USA). Band component analysis was undertaken using the Jandel 'Peakfit' software package, which enabled the type of fitting, function to be selected and allows specific parameters to be fixed or varied accordingly. Band fitting was done using a Gauss-Lorentz cross-product function with the minimum number of component bands used for the fitting process. The Gauss-Lorentz ratio was maintained at values greater than 0.7 and fitting was undertaken until reproducible results were obtained with squared correlations of r^2 greater than 0.995.

RESULTS AND DISCUSSION

The basic copper sulphate minerals antlerite, brochantite, posnjakite and langite all contain OH groups which are hydrogen bonded to adjacent sulphate groups (Araki, 1961; Galy et al., 1984; Gentsch and Weber, 1984; Helliwell and Smith, 1997; Mellini and Merlino, 1979). The minerals posnjakite and langite contain water molecules which are also involved in hydrogen bonding with the adjacent sulphate anions. Antlerite has four OH units in the structure; brochantite has six OH units, and therefore Raman spectroscopy enables the spectra of some of these units to be obtained. Both antlerite and brochantite have hydroxyl stretching bands at 3580 and 3480 cm^{-1} as is shown in Figure 1. Posnjakite and langite are hydrated congeners of brochantite and hence additional bands in their spectra over and above those observed in the spectra of antlerite and brochantite are attributable to water OH stretching bands. Wroewulfite is a dimorph of langite. Bands are observed for langite at 3405 , 3372 and 3262 cm^{-1} and are assigned to these water vibrations. Two hydroxyl OH stretching bands are observed at 3564 and 3588 cm^{-1} . Bouchard-Abouchacra reported the Raman spectrum of brochantite and observed bands at 3562 and 3585

cm⁻¹ (Bouchard-Abouchacra, 2001). However, in the spectrum reported by Bouchard for brochantite additional bands were observed at 3370 and 3400 cm⁻¹ (Bouchard-Abouchacra, 2001). The spectrum corresponds to that of langite and water bands are observed in the spectrum. The Raman spectrum reported for antlerite shows hydroxyl stretching bands at 3488 and 3580 cm⁻¹.

Studies have shown a strong correlation between OH stretching frequencies and both O··O bond distances and H··O hydrogen bond distances (Emsley, 1980; Lutz, 1995; Mikenda, 1986; Novak, 1974). Libowitzky (1999) based upon the hydroxyl stretching frequencies as determined by infrared spectroscopy, showed that a regression function can be employed relating the above correlations with regression coefficients better than 0.96 (Libowitzky, 1999).

The function is $\nu_1 = 3592 - 304 \times 10^9 \exp(-d(\text{O-O})/0.1321) \text{ cm}^{-1}$.

Table 1 reports the hydrogen bond distances for the basic sulphate minerals as calculated using available X-ray diffraction data, together with the calculated OH stretching frequencies and those observed by Raman spectroscopy. For antlerite, four hydrogen bonds are observed with distances of 3.188, 3.230, 2.971 Å. By using the above equation predicted OH stretching frequencies of 3582, 3585 and 3540 cm⁻¹ are obtained. The observed hydroxyl stretching frequencies are 3580 and 3488 cm⁻¹. The spectrometer cannot separate the two predicted bands at 3582 and 3580 cm⁻¹ and these will be observed as one band. The observed band at 3488 cm⁻¹ does not match well with the predicted value of 3540 cm⁻¹. The reason for this mismatch is attributed to a bifurcated bond. A second reason for the mismatch is the bending of hydrogen bonds. Such bonding is not necessarily linear. For brochantite six hydrogen bonds are observed with distances of 2.694, 3.131 (bifurcated), 3.059, 2.868, 2.919 and 3.021 Å. The last OH(6) group is not hydrogen bonded. The hydrogen bond distance of 2.694 Å predicts an OH stretching frequency of 3169 cm⁻¹. This band is not observed. Raman spectra are highly orientation dependent. It is possible that this band was not observed for this reason. Hydrogen bond provides a predicted stretching frequency of 3565 cm⁻¹, which is close to that observed at 3580 cm⁻¹.

There are some 8 hydrogen bonds that can be predicted for the structure of wroewulfite (Table 1). The O··O values all lie in the range 2.72 to 2.99 Å. It should

also be noted that not all hydrogen atoms from OH units or water molecules form hydrogen bonds (bonds g, h and i). Hydrogen bond (a) is of distance 2.72 Å, which, by using the Libowitzky type function, predicts a hydroxyl stretching frequency of 3245 cm⁻¹. This band is observed at 3216 cm⁻¹, in good agreement with the predicted value. The second hydrogen bond (bond (b)) is of 2.99 Å in length and a hydroxyl stretching frequency of 3547 cm⁻¹ is predicted. A band at 3542 cm⁻¹ is observed. Hydrogen bonds (a) and (b) are different in terms of the bond length and what is being distinguished is the strength of the hydrogen bond with bond (a) being strong and bond (b) significantly weaker. Such a distinction may be somewhat arbitrary. Any hydroxyl stretching vibration above 3590 cm⁻¹ results from weak hydrogen bonding. Bond (c) of distance 2.83 Å predicts a value of 3441 cm⁻¹. However there is no observed band in this position. It is possible that the orientation of the crystal was such that differential polarisation vector did not align with the OH bond. The closest band is at 3325 or 3487 cm⁻¹. Bond (d) is 2.94 Å and a frequency of 3526 cm⁻¹ is proposed, and a band is observed at 3542 cm⁻¹. What is also possible is that accidental degeneracy can occur. This accidental degeneracy results from the overlap of bands. The predicted bands combine to form a single broad band, as is observed in Figure 1 for wroewulfite.

The crystal structure of langite has been published but it is difficult to ascertain precise hydrogen bond positions without neutron scattering measurements (Galy et al., 1984; Gentsch and Weber, 1984; Wappler, 1971). The O··O distances are available from X-ray diffraction data. From published data of langite we predict some 13 possible hydrogen bonds and these are listed in Table 1. The system is complex and hydrogen bond distances of 2.770 Å to 3.156 Å (O-O) are calculated. The hydrogen bond distance of 2.770 Å is indicative of a strong hydrogen bond and this predicts hydroxyl stretching frequencies of 3354 cm⁻¹ (hydrogen bond (d)). Hydrogen bond distances of 3.156 Å are indicative of weak hydrogen bonds and predicted frequencies approaching 3579 cm⁻¹ are obtained. Because of the flattening of the Libowitzky function in the high wavenumber region, little differences are observed in the predicted band positions for the weak hydrogen bonds.

In this work we have used the Libowitzky function to ascertain the usefulness for comparing the hydroxyl stretching vibrations and the sulphate SO₄ stretching

vibrations to the O-H and O···O bonding distances. We have then used the positions of the OH stretching vibrations to predict hydrogen bond distances for the OH units in the crystal structure for selected complex sulphates. In this way we calculate the hydrogen bond distances by the use of the Raman hydroxyl stretching bands. The data in Table 1 fundamentally distinguish between types of OH units according to the H···O hydrogen bond distances (Libowitzky, 1999). The table shows a range of hydrogen bond distances. These distances enable the calculation of the hydroxyl stretching band positions. To the best of our knowledge, no neutron diffraction or X-ray diffraction studies of these minerals has been forthcoming and hence no hydrogen bond H···O distances published. In this set of data, hydroxyl stretching frequencies of the Raman spectra have been used to predict the hydrogen bond distances for these minerals and by using the band width of the hydroxyl stretching frequencies estimates of the variation in the hydrogen bond distances predicted. No further attribution of the bonds can be made as the structures have not been determined.

The Raman spectra of the hydroxyl stretching region of the selected multi-anionic minerals devilline, cyanotrichite, glaucocerinite, serpierite and ktenasite are shown in Figure 2. Spectroscopic analysis of the data is reported in Table 2. The complex copper sulphates contain two types of units capable of hydrogen bonding namely the water molecule and the hydroxyl group. Three OH stretching vibrations are observed in the Raman spectra of devilline at 3501, 3458 and 3456 cm^{-1} . The halfwidth values for these bands are 61.9, 16.4 and 87.0 cm^{-1} , respectively. The predicted hydrogen bond distances for the devilline mineral are 2.89₇, 2.84₆ and 2.84₃ Å. No neutron data are available for comparison with these predicted values. Variation in the hydrogen bond distances are ± 0.015 , 0.009 and 0.517 Å, respectively. For cyanotrichite, four hydroxyl stretching bands are observed at 3590, 3476, 3398 and 3198 cm^{-1} . Thus hydrogen bonds are predicted to be 3.40₁, 2.86₅, 2.79₇ and 2.70₀ Å. It appears that the hydrogen bonds may be divided into strong and weak hydrogen bonds according to the bond distance. Bonds of distance greater than 2.8 Å may be described as weak hydrogen bonds and bonds less than 2.8 Å as strong hydrogen bonds. The bandwidth of the Raman band indicates the variation in hydrogen bond distance. The band width of 59.0 cm^{-1} for the first OH stretching band at 3590 cm^{-1} means that the variation in bond distance is $\pm 0.36_4$ Å. Greater variation is observed for the weak hydrogen bonds. The band at 3198 cm^{-1} attributed to a water

OH stretching vibration is broad with a bandwidth of 423 cm^{-1} . This means the variation in bond distance of $\pm 0.65_3\text{ \AA}$.

The complex sulphate mineral glaucocerinite shows two OH stretching vibrations at 3471 and 3238 cm^{-1} with bandwidths of 235 and 450 cm^{-1} . This results in hydrogen bond distances of 3.980 and 2.717 \AA with variation of ± 0.653 and $\pm 0.133\text{ \AA}$ respectively. Again two types of hydrogen bonds are distinguished according to the bond distance, namely weak (3.980 \AA) and strong (2.717 \AA) hydrogen bonds. Greater variation in bond distance is observed for the weak hydrogen bonds. For the mineral serpierite, four hydroxyl stretching bands are observed at 3607 , 3558 , 3376 and 3198 cm^{-1} with bandwidths of 23.8 , 85.5 , 226 , 269 cm^{-1} . Hence hydrogen bond distances of 3.44_5 , 3.026_9 , 2.78_0 and 2.70_0 are predicted. For ktenasite, five hydroxyl stretching bands are observed at 3603 , 3554 , 3465 , 3348 and 3187 cm^{-1} resulting in hydrogen bond distances of 3.54_0 , 3.01_0 , 2.85_7 , 2.76_6 and 2.69_9 \AA .

Sulphate bands:

The Raman spectroscopy of the aqueous sulphate tetrahedral oxyanion yields the symmetric stretching (ν_1) vibration at 981 cm^{-1} , the symmetric bending (ν_2) mode at 451 cm^{-1} , the antisymmetric stretching (ν_3) mode at 1104 cm^{-1} and the antisymmetric bending (ν_4) mode at 613 cm^{-1} (Frost et al., 2003). The Raman spectrum of the mineral chalcantite shows a single symmetric stretching mode at 984.7 cm^{-1} . Two ν_2 modes are observed at 463 and 445 cm^{-1} and three ν_3 modes at 1173 , 1146 and 1100 cm^{-1} . The ν_4 mode is observed as a single band at 610 cm^{-1} . A complex set of overlapping bands is observed in the low wavenumber region with broad bands observed at 257 , 244 , 210 136 and 126 cm^{-1} . Recently, Raman spectra of four basic copper sulphate minerals, namely antlerite, brochantite, posnjakite and langite, were published (Frost et al., 2003). The SO symmetric stretching modes for the four basic copper sulphate minerals are observed at 985 , 990 , 972 and 974 cm^{-1} respectively. Only the mineral brochantite showed a single band in this region. The Raman spectrum of antlerite shows bands at 990 , 985 and 902 cm^{-1} ; whilst posnjakite has bands at 972 and 905 cm^{-1} . Langite Raman spectrum shows complexity with

overlapping bands observed at 982, 974 and 911 cm^{-1} . The observation of more than one symmetric SO_4 stretching vibration is attributed to a reduction in T_d symmetry. It should also be noted that each of the minerals displays a band(s) at around 1906 cm^{-1} . This band is attributed to the first overtone of the ν_1 symmetric stretching vibrations. Two bands are observed for langite at 1911 and 1906 cm^{-1} .

The two minerals posnjakite and langite show considerable complexity in the SO_4 antisymmetric stretching region whilst antlerite and brochantite show some similarity, which is not unexpected since their stoichiometry is similar. The Raman spectrum of chalcantite has the most intense band in this spectral region centred at 1146 cm^{-1} . The Raman spectrum of antlerite shows bands at 1173, 1134 and 1078 cm^{-1} with the latter band being the most intense. A broad band centred on 1266 cm^{-1} is also observed for each of the minerals. The Raman spectrum of brochantite displays bands at 1173, 1135 and 1078 cm^{-1} . The Raman spectra of posnjakite and langite are very different from that of the former two minerals with a complex set of overlapping bands. The Raman spectrum of posnjakite shows bands at 1147, 1153, 1132, 1105 and 1078 cm^{-1} in the antisymmetric stretching region. In addition, bands are also observed at 1271 and 1251 cm^{-1} . A further band is observed at around 1370 cm^{-1} . This band is common to all the spectra of these basic copper sulphate minerals. The band is of very low intensity for antlerite, brochantite and chalcantite. Raman bands for langite are observed at 1266, 1172, 1149, 1128, 1102 and 1076 cm^{-1} .

The Raman spectra of the SO_4 symmetric and antisymmetric stretching vibrations of the complex copper sulphates are shown in Figure 3. The results of the Raman spectroscopic analyses are shown in Table 2. The Raman spectrum of devilline shows a single SO_4 symmetric stretching bands at 1007 cm^{-1} . The band is sharp with a bandwidth of 3.1 cm^{-1} . The antisymmetric stretching band for devilline is observed at 1134 cm^{-1} . In contrast, the Raman spectrum of cyanotrichite shows a single intense band at 976 cm^{-1} with a broad low intensity band at 960 cm^{-1} . Three antisymmetric stretching bands are observed at 1137, 1101 and 1057 cm^{-1} . For glaucocerinite bands are observed at 1007 and 981 cm^{-1} for the symmetric stretching bands and at 1129 and 1059 cm^{-1} for the antisymmetric stretching vibrations. For

serpierite a single symmetric stretching mode at 988 cm^{-1} is observed and three antisymmetric stretching bands are observed at 1131 , 1122 and 1077 cm^{-1} . For ktenasite, multiple symmetric stretching bands are observed at 994 , 981 and 973 cm^{-1} .

It is noted that the peak position of the sulphate band varies with the mineral. By selection of the hydrogen bond distances, as predicted from the position of the OH stretching vibration in the Raman spectrum, and plotting versus the SO_4 symmetric stretching band position, a relationship as shown in Figure 4 is obtained. This graph shows quite conclusively that the position of the SO_4 stretching position is simply a function of the hydrogen bond strength as determined by the hydrogen bond distance. Two trends are observed, first for the simple basic copper sulphate minerals and secondly for the complex basic copper sulphate minerals. The two graphs parallel each other.

The complexity of the antisymmetric stretching region is reflected in the spectra of the ν_2 bending region (Figure 5). The spectra of antlerite and brochantite are similar as are those for posnjakite and langite in this spectral region (Frost et al., 2003). The antlerite Raman spectrum shows bands at 485 , 469 , 440 and 415 cm^{-1} with the latter band having the highest intensity. Bouchard-Abouchacra reported bands for antlerite at 483 , 470 , 444 and 416 cm^{-1} in excellent agreement with our data (Bouchard-Abouchacra, 2001). Raman spectra of brochantite are similar except that additional bands at 517 and 501 cm^{-1} are observed. The Raman spectra of posnjakite show bands at 511 , 482 , 447 , 422 , 386 and 363 cm^{-1} . This complex set of bands in this region is also observed for langite with bands observed at 507 , 481 , 449 , 420 , 391 cm^{-1} . The Raman spectrum of wroewulfite shows a complex set of overlapping bands at 472 , 457 , 443 and 415 cm^{-1} . The observation of additional bands over and above that which would be predicted for the sulphate anion (a single band at 451 cm^{-1}), may be attributed to a number of factors including symmetry reduction, local stress in the crystals and crystal orientation effects.

Raman spectra of the mineral phases for this region are different, and each phase has its own characteristic spectrum. For antlerite four Raman bands are observed at 651 , 629 , 606 and 600 cm^{-1} . Bands at 630 and 604 cm^{-1} were found by Bouchard-Abouchacra for antlerite (Bouchard-Abouchacra, 2001). In contrast,

chalcantite showed only a single band at 610 cm^{-1} . The Raman spectrum of brochantite shows bands at 629 , 608 and 600 cm^{-1} . Bands were observed for brochantite by Bouchard at 621 , 611 and 599 cm^{-1} (Bouchard-Abouchacra, 2001). The Raman spectrum of posnjakite shows bands at 621 , 609 and 596 cm^{-1} and langite at 621 , 609 and 596 cm^{-1} . Whilst the bands for posnjakite and langite are in similar positions, the intensity of the bands varies considerably, although this may be a crystal orientation effect. The Raman spectrum of wroewulfeite shows two bands at 621 and 600 cm^{-1} .

The Raman spectra of the low wavenumber region of the selected copper complex minerals are shown in Figure 6 and the results reported in Table 2. Multiple bands are observed in the 400 to 500 cm^{-1} region and are attributed to the ν_2 bending modes. The observation of several bending modes is in agreement with the number of antisymmetric stretching vibrations. Bands are observed at 479 , 443 and 408 cm^{-1} for cyanotrichite, at 450 and 430 cm^{-1} for devilline, 498 and 471 cm^{-1} for glaucocerinite, at 475 , 445 and 421 cm^{-1} for serpierite and at 475 and 449 for ktenasite. The bands in the 500 to 600 cm^{-1} region are attributed to the ν_4 bending modes. Bands below 400 cm^{-1} are attributed to lattice modes. The Raman spectrum of ktenasite shows a single peak in the ν_4 region at 604 cm^{-1} . The Raman spectrum of devilline shows two low intensity bands at 668 and 617 cm^{-1} ; cyanotrichite two overlapping bands at 594 and 530 cm^{-1} ; the Raman spectrum of glaucocerinite shows two bands at 694 , 613 and 555 cm^{-1} . The complexity of the symmetric and antisymmetric bending region shows a reduction in symmetry for these complex sulphate minerals.

The basic copper sulphate minerals are characterised by the position of the hydroxyl stretching vibrations in the Raman spectrum. In addition the minerals posnjakite and langite displayed four water OH stretching vibrations. By using a Libowitzky type function, the hydrogen bond distances were used to predict the hydroxyl stretching frequencies and a comparison made to the observed values. Agreement is excellent. The position of the hydroxyl stretching bands of the complex copper sulphate minerals was used to estimate the hydrogen bond distances in the mineral structures. A comparison was made between these hydrogen bond distances and the position of the SO_4 symmetric stretching vibration.

ACKNOWLEDGMENTS

The infra-structure support of the Inorganic Materials Research Program of the Queensland University of Technology School of Physical and Chemical Sciences is gratefully acknowledged. The Australian Research Council (ARC) is thanked for funding. Prof Allan Pring of the South Australian Museum is thanked for the loan of the basic complex copper sulphate minerals, as is also Mr. Ross Pogson of the Australian Museum. Mr. Dermot Henry of Museum Victoria is thanked for providing basic copper sulphate minerals, chiefly from Australian sources.

The authors wish to thank Eugen Libowitzky for his review of this manuscript and his most helpful and worthwhile comments.

REFERENCES:

- Araki, T. (1961) Crystal structure of antlerite. *Mineralogy Journal* (Tokyo), 3, 233-35.
- Bersani, D., Antonioli, G., Lottici, P.P., Fornari, L. and Castrichini, M. (2001) Restoration of a Parmigianino's fresco: a micro-Raman investigation of the pictorial surface. *Proceedings of SPIE-The International Society for Optical Engineering*, 4402, 221-226.
- Bouchard-Abouchacra, M. (2001) Evaluation des capacités de la Microscopie Raman dans la caractérisation minéralogique et physicochimique de matériaux archéologiques: métaux, vitraux & pigments. PhD Thesis.
- Crane, M., Frost, R.L., Williams, P.A. and Kloprogge, J.T. (2002) Raman spectroscopy of the molybdate minerals chillagite (tungsteinian wulfenite-14), stolzite, scheelite, wolframite and wulfenite. *Journal of Raman Spectroscopy*, 33, 62-66.
- Dunn, P.J., Rouse, R.C. and Nelen, J.A. (1975) Wroewolfeite, a new copper sulfate hydroxide hydrate. *Mineralogical Magazine*, 40, 1-5.
- Effenberger, H. (1985) The crystal structure of mammothite, $\text{Pb}_6\text{Cu}_4\text{AlSbO}_2(\text{OH})_{16}\text{Cl}_4(\text{SO}_4)_2$. *TMPM, Tschermaks Mineral. Petrogr. Mitt.*, 34, 279-88.
- Effenberger, H. (1988) Ramsbeckite, $(\text{Cu,Zn})_{15}(\text{OH})_{22}(\text{SO}_4)_4 \cdot 6\text{H}_2\text{O}$: Revision of the chemical formula based on a structure determination. *Neues Jahrbuch fuer Mineralogie, Monatshefte*, 38-48.
- Effenberger, H. and Zemmann, J. (1984) The crystal structure of caratiite. *Mineralogical Magazine*, 48, 541-6.
- Emsley, J. (1980) Very strong hydrogen bonding. *Chemical Society Reviews*, 9, 91-124.
- Finney, J.J. and Araki, T. (1963) Refinement of the crystal structure of antlerite. *Nature*, 197, 70.
- Fowles, G. (1926) Basic copper sulfates. *Journal of the Chemical Society*, 1845-58.
- Frost, R.L., Kloprogge, J.T., Williams, P.A. and Leverett, P. (2000) Raman microscopy of some natural pseudo-alums: halotrichite, apjohnite and wupatkiite, at 298 and 77 K. *Journal of Raman Spectroscopy*, 31, 1083-1087.

- Frost, R.L., Martens, W.N., Rintoul, L., Mahmutagic, E. and Kloprogge, J.T. (2002a) Raman spectroscopic study of azurite and malachite at 298 and 77 K. *Journal of Raman Spectroscopy*, 33, 252-259.
- Frost, R.L., Williams, P.A., Kloprogge, J.T. and Leverett, P. (2001) Raman spectroscopy of descloizite and mottramite at 298 and 77 K. *Journal of Raman Spectroscopy*, 32, 906-911.
- Frost, R.L., Williams, P.A., Martens, W., Kloprogge, J.T. and Leverett, P. (2002b) Raman spectroscopy of the basic copper phosphate minerals cornetite, libethenite, pseudomalachite, reichenbachite and ludjibaite. *Journal of Raman Spectroscopy*, 33, 260-263.
- Galy, J., Jaud, J., Pulou, R. and Sempere, R. (1984) Crystal structure of the langite $\text{Cu}_4[\text{SO}_4(\text{OH})_6\text{H}_2\text{O}]\cdot\text{H}_2\text{O}$. *Bulletin de Mineralogie*, 107, 641-8.
- Gentsch, M. and Weber, K. (1984) Structure of langite, $\text{Cu}_4[(\text{OH})_6|\text{SO}_4]\cdot 2\text{H}_2\text{O}$. *Acta Crystallographica, Section C: Crystal Structure Communications*, C40, 1309-11.
- Giuseppetti, G. and Tadini, C. (1987) Corkite, $\text{PbFe}_3(\text{SO}_4)(\text{PO}_4)(\text{OH})_6$, its crystal structure and ordered arrangement of the tetrahedral cations. *Neues Jahrbuch fuer Mineralogie, Monatshefte*, 71-81.
- Helliwell, M. and Smith, J.V. (1997) Brochantite. *Acta Crystallographica, Section C: Crystal Structure Communications*, C53, 1369-1371.
- Hess, H., Keller, P. and Riffel, H. (1988) The crystal structure of chenite, $\text{Pb}_4\text{Cu}(\text{OH})_6(\text{SO}_4)_2$. *Neues Jahrbuch fuer Mineralogie, Monatshefte*, 259-64.
- Kratschmer, A., Odnevall Wallinder, I. and Leygraf, C. (2002) The evolution of outdoor copper patina. *Corrosion Science*, 44, 425-450.
- Libowitzky, E. (1999) Correlation of O-H stretching frequencies and O-H...O hydrogen bond lengths in minerals. *Monatshefte für Chemie*, 130, 1047-1059.
- Livingston, R.A. (1991) Influence of the environment on the patina of the Statue of Liberty. *Environmental Science and Technology*, 25, 1400-8.
- Lobnig, R., Frankenthal, R.P., Jankoski, C.A., Siconolfi, D.J., Sinclair, J.D., Unger, M. and Stratmann, M. (1999) Corrosion and protection of metals in the presence of submicron dust particles. *Proceedings - Electrochemical Society*, 99-29, 97-126.
- Lutz, H. (1995) Hydroxide ions in condensed materials - correlation of spectroscopic and structural data. *Structure and Bonding (Berlin, Germany)*, 82, 85-103.
- Mankowski, g., Duthil, J.P. and Giusti, A. (1997) The pit morphology on copper in chloride- and sulfate-containing solutions. *Corrosion Science*, 39, 27-42.
- Matsuda, S., Aoki, S. and Kawanobe, W. (1997) Analysis of corrosion products formed on the bronze garden lantern of Todaiji Temple in Nara. *Hozon Kagaku*, 36, 1-27.
- Mellini, M. and Merlino, S. (1978) Ktenasite, another mineral with $\infty 2[(\text{Cu},\text{Zn})_2(\text{OH})_3\text{O}]$ - octahedral sheets. *Z. Kristallogr., Kristallgeom., Kristallphys., Kristallchem.*, 147, 129-40.
- Mellini, M. and Merlino, S. (1979) Posnjakite: $2[\text{Cu}_4(\text{OH})_6(\text{H}_2\text{O})\text{O}]$ octahedral sheets in its structure. *Z. Kristallogr.*, 149, 249-57.
- Mereiter, K. (1982) The crystal structure of johannite, $\text{Cu}(\text{UO}_2)_2(\text{OH})_2(\text{SO}_4)_2\cdot 8\text{H}_2\text{O}$. *Tschermaks Mineralogische und Petrographische Mitteilungen*, 30, 47-57.
- Mikenda, W. (1986) Stretching frequency versus bond distance correlation of O-D(H)...Y (Y = N, O, S, Se, Cl, Br, I) hydrogen bonds in solid hydrates. *Journal of Molecular Structure*, 147, 1-15.

- Nord, A.G., Mattsson, E. and Tronner, K. (1998) Mineral phases on corroded archaeological bronze artifacts excavated in Sweden. *Neues Jahrbuch fuer Mineralogie, Monatshefte*, 265-277.
- Novak, A. (1974) Hydrogen bonding in solids. Correlation of spectroscopic and crystallographic data. *Structure and Bonding (Berlin)*, 18, 177-216.
- Orlandi, P. and Perchiazzi, N. (1989) Ramsbeckite, $(\text{Cu,Zn})_{15}(\text{OH})_{22}(\text{SO}_4)_4 \cdot 6\text{H}_2\text{O}$, a first occurrence for Italy from "La Veneziana" mine, Valle dei Mercanti, Vicenza. *Eur. J. Mineral.*, 1, 147-9.
- Pierrot, R. and Sainfeld, P. (1961) Devillite and spangolite of Corsica. The associated minerals. *Bulletin De La Societe Francaise Mineralogie Et De Cristallographie*, 84, 90-1.
- Pollard, A.M., Thomas, R.G. and Williams, P.A. (1990) Mineralogical changes arising from the use of aqueous sodium carbonate solutions for the treatment of archaeological copper objects. *Studies in Conservation*, 35, 148-52.
- Richmond, W.E. and Wolfe, C.W. (1940) Crystallography of dolerophanite. *American Mineralogist*, 25, 606-10.
- Ruesenberg, K.A. and Paulis, P. (1996) Conversions and new formations in slag dumps of the Příbram lead and silver foundry, Czech Republic. *Aufschluss*, 47, 267-287.
- Ungemach, H. (1924) Antlerite. *Bulletin De La Societe Francaise Mineralogie Et De Cristallographie*, 47, 124-9.
- Vergasova, L.P., Filatov, S.K., Serafimova, E.K. and Semenova, T.F. (1988) Ponomarevite, $\text{K}_4\text{Cu}_4\text{OCl}_{10}$ - a new mineral from volcanic sublimations. *Doklady Akademii Nauk*, 300, 1197-200.
- Vergasova, L.P., Filatov, S.K., Serafimova, E.K. and Starova, G.L. (1984) Piypite, $\text{K}_2\text{Cu}_2\text{O}(\text{SO}_4)_2$ - a new mineral of volcanic sublimates. *Doklady Akademii Nauk*, 275, 714-17.
- Von Hodenberg, R., Krause, W. and Taeuber, H. (1984) Schulenbergite, $(\text{Cu,Zn})_7(\text{SO}_4,\text{CO}_3)_2(\text{OH})_{10} \cdot 3\text{H}_2\text{O}$, a new mineral. *Neues Jahrbuch fuer Mineralogie, Monatshefte., Monatsh.*, 17-24.
- Wappler, G. (1971) Crystal structure of langite $\text{Cu}_4[(\text{OH})_6/\text{SO}_4] \cdot \text{H}_2\text{O}$. *Berichte der Deutschen Gesellschaft Geologische Wissenschaften Reihe B*, 16, 175-203.
- Wappler, G. and Tischendorf, G. (1980) Identification of some secondary minerals from the dumps of the Friedrichsglueck Mine, near Neustadt/Rennsteig [East Germany]. *Zeitschrift Fur Geologische Wissenschaften*, 8, 1397-402.
- Zubkova, N.V., Pushcharovsky, D.Y., Giester, G., Tillmanns, E., Pekov, I.V. and Kleimenov, D.A. (2002) The crystal structure of arsentsumebite, $\text{Pb}_2\text{Cu}[(\text{As}, \text{S})\text{O}_4]_2(\text{OH})$. *Mineralogy and Petrology*, 75, 79-88.

	Bond	Hydrogen bonds	$\nu_1(\text{calc})$	$\nu_1(\text{obs})$
antlerite	a	OH(1)-O(3) 3.188(5) Å	3582	3580**
	b	OH(2)-O(3) 3.230(5) Å	3585	3580**
	c	OH(3)-O(3) 2.971(5) Å*	3540	3488
	d	OH(3)-O(1) 3.136(5) Å*		
brochiantite	a	OH(1)-O(8) 2.694 Å*	3169	*
	b	OH(1)-O(9) 3.131 Å*	3565	3580**
	c	OH(3)-O(9) 3.059 Å	3579	3489
	d	OH(2)-O(6) 2.868 Å	3515 <i>f</i>	3501 <i>f</i>
	e	OH(4)-O(9) 2.919 Å	3556 <i>f</i>	3501 <i>f</i>
	f	OH(5)-O(9) 3.021 Å	3590	3580**
	g	OH(6) is not H-bonded		
posnjakite	a	OH(1)-O(11) 2.746 Å	3307	3372
	b	OH(2)-O(10) 2.732 Å	3275	3262**
	c	OH(3)-O(9) 3.047 Å	3563	3564
	d	OH(4)-O(11) 2.715 Å	3231	3262**
	e	OH(6)-O(9) 2.737 Å	3287	3262**
	f	OH(8)-O(10) 2.872 Å O(8) is the water molecule	3482	3405
	g	OH(8)-O(11) 3.189 Å	3582	3588 <i>f</i>
	h	OH(5) is not H-bonded	3590	3588 <i>f</i>
wroewulfite	a	OH(5)-O(12) 2.72 Å	3245	3216
	b	OH(7)-O(2) 2.99 Å	3547	3542**
	c	OH(9)-O(4) 2.83 Å	3441	3325?
	d	OH(6)-O(1)* 2.94 Å	3526	3487
	e	OH(6)-O(2)* 2.87 Å	3441	3325?
	f	OH(8)-O(3) 2.9 Å	3503	3485
	g	OH(10) not H-bonded	3590	3542
	h	Neither H on water O(11) is H- bonded	3590	3542
	i	One H on water O(12) is not H- bonded	3590	3542
langite	a	O(1)-O(9) 2.850 Å	3462	
	b	O(1)-O(12) 3.115 Å	3575	3564 or 3587
	c	O(1)-O(8) 3.156 Å	3579	3564 or 3587
	d	O(3)-O(12) 2.770 Å	3354	3372
	e	O(3)-O(6) 2.777 Å	3366	3372
	f	O(3)-O(7)* 2.972 Å	3540	3564
	g	O(4)-O(7)* 3.078 Å	Not to be seen; bifurcation	
	h	O(4)-O(11) 2.889 Å	3495	3564?
	i	O(4)-O(12) 2.884 Å	3492	3564?
	j	OH not bonded	3592	3587
	k	O(10)-O(12)** 2.725	3258	3260
	l	a. O(10)-O(11)** 3.098 Å	Not to be seen; bifurcation	

	m	b. O(11)-O(12) 2.869 Å	3480	3405
		NOTE O(5) to O(10) are OH groups; O(11) and O(12) are water molecules. The former is bonded to a copper and the latter is a hydrogen-bonded lattice water molecule.		

*Bifurcated; spectroscopic manifestation expected from the shorter interaction.

**Overlapped. f overlapped

Table 1 Predicted Raman band frequencies of the hydroxyl stretching vibrations based upon the hydrogen bond distances.

Mineral	Suggested hydrogen bond origin#	Observed Raman band positions (cm ⁻¹)	Estimated hydrogen bond distance (Å)	Observed Raman band width (cm ⁻¹)	Estimated hydrogen bond distance variation (Å)
devilline	OH 1	3501	2.89 ₇	61.9	± 0.01 ₅
	OH 2	3458	2.84 ₆	16.4	± 0.009
	H ₂ O 1	3456	2.84 ₃	87.0	± 0.051 ₇
cyanotrichite	OH 1	3590	3.40 ₁	59.0	± 0.364
	OH 2	3476	2.86 ₅	59.0	± 0.038 ₄
	H ₂ O 1	3398	2.79 ₇	92.9	± 0.036
	H ₂ O 2	3198	2.70 ₀	423.7	± 0.10 ₅
glaucozerinite	OH 1	3471	2.86 ₅	235.0	± 0.065 ₃
	H ₂ O 1	3238	2.71 ₇	450.0	± 0.133
serpierite	OH 1	3607	3.44 ₅	23.8	± 0.100
	OH 2	3558	3.40 ₁	85.5	± 0.108
	H ₂ O 1	3376	2.78 ₀	226.2	± 0.146 ₄
	H ₂ O 2	3198	2.70 ₀	268.9	± 0.035 ₆
	OH 1	3603	3.44 ₁	24.7	± 0.01 ₅

ktenasite	OH 2	3554	3.01	47.4	± 0.129
	H ₂ O 1	3465	2.85 ₇	76.4	± 0.043
	H ₂ O 2	3348	2.76 ₆	24.7	± 0.007
	H ₂ O 3	3187	2.69 ₉	27.5	± 0.060

Assignments made according to the hydroxyl stretching wavenumber in the raman spectra.

Table 2 Correlation between hydroxyl stretching frequencies and estimated hydrogen bond distances.

Table 3 Raman spectroscopic analysis of some complex copper(II) sulphate minerals

Devilline CaCu₄(SO₄)₂(OH)₆·3H₂O	Cyanotrichite Cu₄Al₂SO₄(OH)₁₂·2H₂O	Glaucozerinite (Zn,Cu)₁₀Al₆(SO₄)₃(OH)₃₂·18H₂O	Serpierite Ca(Cu,Zn)₄(SO₄)₂(OH)₆·3H₂O	Ktenasite (Cu,Zn)₅(SO₄)₂(OH)₆·6H₂O
3501	3590	3471	3607	3603
3458	3476	3238	3558	3554
3456	3398		3376	3465
	3198		3198	3348
1134	1137	1129	1131	1111
	1101	1059	1122	1060
	1057		1077	
1007	976	1007		994
989		981	988	981
898	828		843	973
857	829		806	710
796	789		769	
668	594	694	645	604
617	530	613	605	
	510	555		
479	450	498	475	475
443	430	471	445	449
408			421	
324	365	256	332	397
	331		250	332
	277			
237	230	193	217	223
	195	160	169	162

List of tables

Table 1 Predicted Raman band frequencies of the hydroxyl stretching vibrations based upon the hydrogen bond distances.

Table 2 Correlation between hydroxyl stretching frequencies and estimated hydrogen bond distances.

Table 3 Raman spectroscopic analysis of some complex copper(II) sulphate minerals

List of Figures

Figure 1 Raman spectrum of the hydroxyl stretching region of (a) antlerite (b) brochantite (c) posnjakite (d) langite (e) wroewulfite

Figure 2 Raman spectrum of the hydroxyl stretching region of (a) cyanotrichite (b) devilline (c) glaucocerinite (d) serpierite (e) ktenasite

Figure 3 Raman spectrum of the SO₄ stretching region of (a) cyanotrichite (b) devilline (c) glaucocerinite (d) serpierite (e) ktenasite.

Figure 4 Hydrogen bond distance as a function of the peak position of the symmetric SO₄ stretching vibration.

Figure 5 Raman spectrum of the SO₄ bending region of (a) antlerite (b) brochantite (c) posnjakite (d) langite (e) wroewulfite

Figure 6 Raman spectrum of the low wavenumber region of (a) cyanotrichite (b) devilline (c) glaucocerinite (d) serpierite (e) ktenasite.

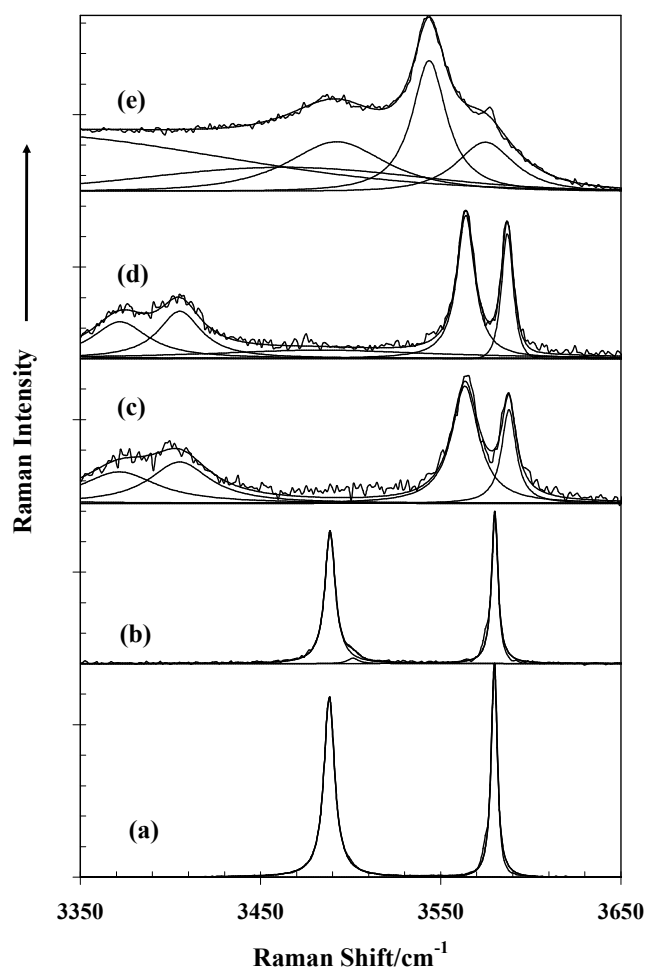


Figure 1

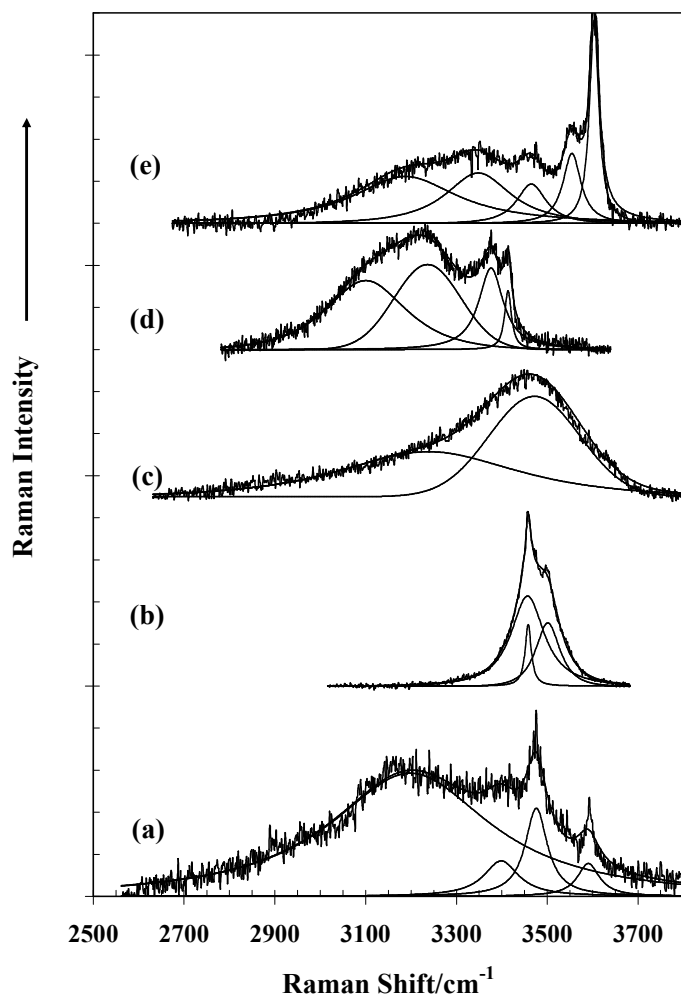


Figure 2

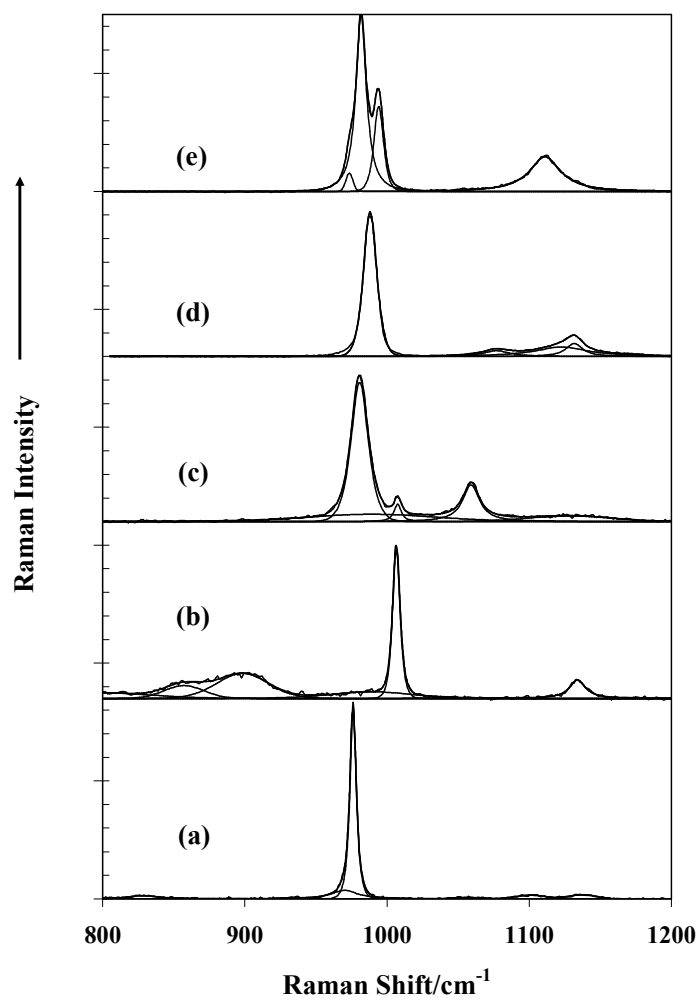


Figure 3

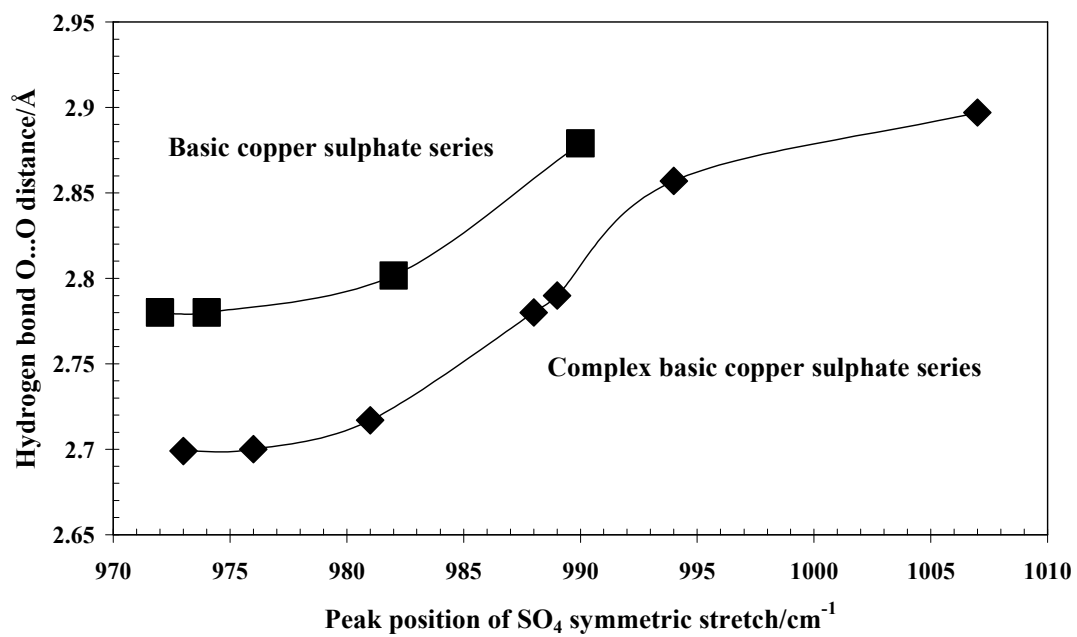


Figure 4

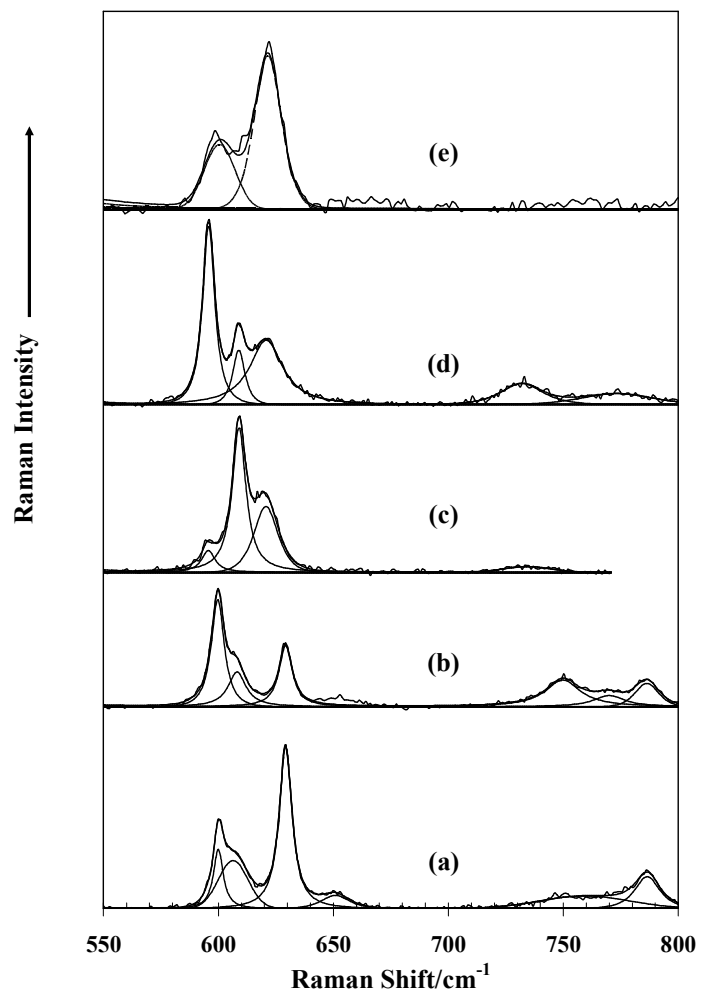


Figure 5

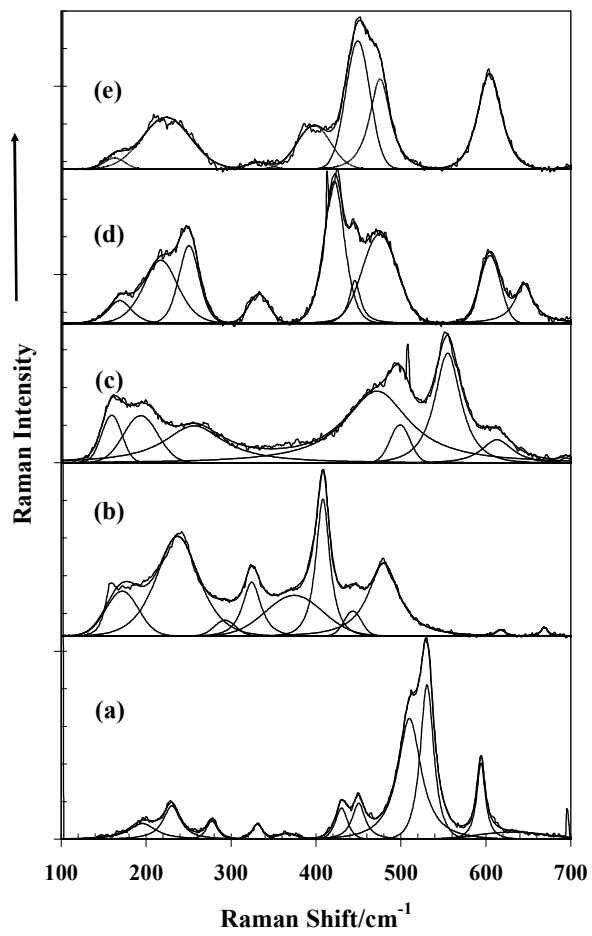


Figure 6